Inorg. Chem. **2008**, *47*, 4310−4318

Modulating Affinities of Di-2-picolylamine (DPA)-Substituted Quinoline Sensors for Zinc Ions by Varying Pendant Ligands

Lin Xue,[†,‡] Huan-Huan Wang,[†,‡] Xiao-Jun Wang,[§] and Hua Jiang*[,†]

Beijing National Laboratory for Molecular Sciences, CAS Key Laboratory of Photochemistry, Institute of Chemistry, Chinese Academy of Sciences, Beijing, 100190, People's Republic of China, Graduate School of Chinese Academy of Sciences, Beijing, 100049, People's Republic of China, and Department of Chemistry, Capital Normal University, Beijing, 100037, People's Republic of China

Received December 11, 2007

We have developed a series of di-2-picolylamine (DPA)-substituted quinoline sensors, **HQ1–4**, bearing a pendant ligand at the 8 position of quinoline. UV–vis spectra of **HQ1–4** showed similar variations to that of **HQ5** but with different varying extents upon the titration of zinc ions. Fluorescence intensities of **HQ1**, **HQ3**, and **HQ4** were enhanced 4–6 times upon the addition of 1 equiv of zinc ions under an aqueous buffer. Somewhat unexpectedly, **HQ2** is nonfluorescent in the presence of metal ions, including zinc ions. The affinities of **HQ** sensors are distributed in a broad range from nanomolarity to femtomolarity by varying the pendant ligands near the coordination unit. More importantly, these new sensors exhibited very high selectivity for Zn^{2+} over Na^{+}, K^{+}, Mg^{2+}, and Ca^{2+} at the millimolar level and over other transition metal ions at the micromolar level, except for Cd^{2+}. These findings indicated that the incorporations of the pendant groups exerted no effect on the spectroscopic properties and selectivity of the parent fluorescent sensor, with the exception of **HQ2**. Finally, X-ray crystal structures of **ZnHQ**'s revealed that the auxiliary pendant groups at the 8 position participated in zinc coordination and were able to tune the affinities of **HQ** sensors.

Introduction

Research on zinc has attracted significant attention since zinc plays major roles in many vital biological processes as structural and catalytic cofactors, neural signal transmitters or modulators, and regulators of gene expression and apoptosis.[1,2] Though it is generally believed that the majority of zinc ions are tightly bound in proteins and enzymes, "free" zinc ions still exist in most cells, where their concentration varies from the subfemtomolar range in bacterial cells to the millimolar range in some vesicles.[3] Up to now, the biological roles of the zinc ion are not well-understood, in part, because of its "nonproperties"[4] such as its colorlessness and being spectroscopic- or magnetic-silent, originating from its d^{10} electron configuration,[5] and in part because of the lack of versatile analyzing tools to visualize zinc ion concentrations over several orders of magnitude.

Due to high sensitivity, fluorescence sensors have been widely used to detect metal ions of biological and environmental interests. Especially, over the past few years, fluorescent sensors for zinc ions have been elbowing their way to center stage in the field of molecular recognition. Numerous zinc sensors based on quinoline, fluorescein, coumarin, peptide, and proteins with apparent dissociation constants in the nanomolar range or higher have been

* Author to whom correspondence should be addressed. E-mail: hjiang@iccas.ac.cn.
† Chinese Academy of Sciences.
‡ Graduate School of Chinese Academy of Sciences.
§ Capital Normal University.

(1) Vallee, B. L.; Falchuk, K. H. *Physiol. Rev.* **1993**, *73*, 79.
(2) (a) Berg, J. M; Shi, Y. *Science* **1996**, *271*, 1081. (b) Special issue on zinc chemistry: *Biometals*, **2001**, *14*. (c) Xie, X.; Smart, T. G. *Nature* **1991**, *349*, 521.
(3) (a) Outten, C. E.; O'Halloran, T. V. *Science* **2001**, *292*, 2488. (b) Finney, L. A.; O'Halloran, T. V. *Science* **2003**, *300*, 931. (c) Frederickson, C. J.; Koh, J. Y.; Bush, A. I. *Nat. Rev. Neurosci.* **2005**, *6*, 449.
(4) Vahrenkamp, H. *Dalton Trans.* **2007**, 4751.
(5) Lim, N. C.; Freake, H. C.; Brückner, C. *Chem.—Eur. J.* **2005**, *11*, 38.
(6) (a) Recent reviews on zinc fluorescent sensors: Kimura, E.; Aoki, S. *Biometals* **2001**, *14*, 191. (b) Hirano, T.; Kikuchi, K.; Nagano, T. *Rev. Fluorescence* **2004**, *1*, 55. (c) Kikuchi, K.; Komatsu, K.; Nagano, T. *Curr. Opin. Chem. Biol.* **2004**, *8*, 182. (d) Jiang, P.; Guo, Z. *Coord. Chem. Rev.* **2004**, *248*, 205. (e) Thompson, R. B. *Curr. Opin. Chem. Biol.* **2005**, *9*, 526. (f) Carol, P.; Sreejith, S.; Ajayaghosh, A. *Chem. Asian J.* **2007**, *2*, 338. (g) Dai, Z.; Canary, J. W. *New J. Chem.* **2007**, *31*, 1708.
(7) Komatsu, K.; Kikuchi, K.; Kojima, H.; Urano, Y.; Nagano, T. *J. Am. Chem. Soc.* **2005**, *127*, 10197.

10.1021/ic702393z CCC: $40.75
Published on Web 04/15/2008

Chart 1. Structures of Sensors Based on 8-Hydroxyquinoline Platform[a]

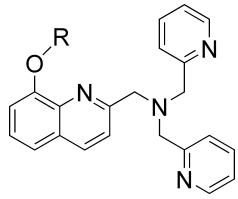

HQ1, R = benzyl
HQ2, R= H
HQ3, R = 2-picolyl
HQ4, R = n-$C_3H_6CO_2Na$
HQ5, R= CH_2CO_2Na

[a] **HQ5** has been previously reported.[12] The others are newly synthesized.

designed and reported.[5,6] Considering the broad range of zinc concentrations in cells, these sensors are still unable to satisfy detecting demands because, if dissociation constants K_d are above the concentrations of zinc in the target samples, the sensors yield no detectable signals. Conversely, if dissociation constants K_d are below the concentrations of zinc in the target samples, the sensors generate saturated signals, which consequently result in losing dynamic information about the interesting regions. Thus, an ideal sensor should have a compatible K_d with the concentration of zinc ions in the target regions. To address this issue, therefore, several families of zinc sensors capable of tuning affinities have been developed, for example, the ZnAF family of sensors described by Nagano et al.,[7] the Zinpyr family described by Lippard and Goldsmith,[8] the benzimidazole sensors described by Fahrnir et al.,[9] peptide scaffolds described by Imperiali et al.,[10] and protein sensors described by Merkx et al. as well.[11] However, most sensors are suitable for detecting free zinc concentration in the micromolar to nanomolar range, with the exception of protein sensors which are able to measure free zinc concentration in the picomolar to femtomolar range.[11b] Thus, it is rather desirable to develop small molecular sensors with various affinities down to the subnanomolar range, or lower. Yet, designing small molecular sensors able to detect the free zinc concentration over an extremely low range is still a challenging task.

We recently showed an extremely sensitive zinc fluorescent sensor with affinity in the subfemtomolar range under physiological conditions (Chart 1, **HQ5**).[12] In this sensor, the di-2-picolylamine (DPA) moiety was adopted as a zinc ion chelator because it is able to afford an excellent selectivity for Zn^{2+} over Na^+, K^+, Mg^{2+}, and Ca^{2+}.[7,8,13] In addition, the amino nitrogen of the DPA group is a good candidate as an electron donor in either photoinduced electron transfer or photoinduced charge transfer (PET or PCT) sensors.[14] 8-Hydroxyquinoline (**8-HQ**), a traditional fluorogenic agent for analyzing Zn^{2+} and other metal ions,[15] was used as a fluorescent platform. We reasoned that the zinc affinity of our reported sensor (**HQ5**) could be further tuned by varying pendant groups at the 8 position of **HQ**. Our strategy is to introduce an assistant chelating group near the coordination unit and, consequently, to achieve a new family of zinc sensors with distinct affinities. In the present context, we wish to present a new series of fluorescent sensors with tunable and very high affinities for zinc ions acquired in this strategy (Chart 1).

Experimental Section

Materials and Methods. Acetone, SeO_2, $NaB(OAc)_3H$, K_2CO_3, 2-chloromethyl pyridine hydrochloride, benzyl bromide, 1,4-dioxane, and metal salts were purchased from Alfa Aesar and used as received. Dimethyl sulfoxide (DMSO) was distilled from CaH_2 under a vacuum and subsequently dried over 3 Å molecular sieves. Compounds **2** and **5** were prepared according to known procedures.[16]

^1H and ^{13}C NMR spectra were recorded on a Bruker DRX-300 or AVANCE-400 spectrometer and referenced to internal tetramethylsilane or solvent signals. UV–vis and fluorescence spectra were measured on a HITACHI 3010 UV–vis spectrometer and a HITACHI F-4500 spectrometer, respectively. Mass spectra (EI, ESI, and MALDI-TOF) were obtained on GCT, LC-MS 2010, and Autotlex III spectrometers, respectively.

Caution! *Perchlorate salts with organic ligands are potentially explosive and should be handled with care.*

General Synthetic Procedures for 3–4. A mixture of 8-hydroxy-2-methylquinoline (**1**) (3.20 g, 20 mmol), alkyl halides (20 mmol), K_2CO_3 (11.06 g, 80 mmol), and KI (1.5 g, 10 mmol) in acetone (60 mL) was refluxed for 24 h. After cooling, the mixture was filtered to remove salts, and the filtrate was evaporated to generate crude residue, which was purified by flash chromatography (silica gel), elueting with methylene chloride containing 0–2% methanol to give the desired products.

8-Pyridylmethyloxy-2-methyl-quinoline (3). Yield: 75%. ^1H NMR ($CDCl_3$, 400 MHz): δ 8.56 (1H, d, J = 3.78 Hz), 7.90−7.86 (1H, m), 7.62−7.53 (2H, m), 7.26−7.17 (3H, m), 7.09 (1H, t, J = 5.20 Hz), 6.99 (1H, d, J = 5.59 Hz), 5.49 (2H, s), 2.76 (3H, s). ^{13}C NMR (100 MHz, $CDCl_3$, ppm): δ 157.36, 156.37, 152.73, 148.33, 139.01, 136.11, 135.40, 126.99, 124.87, 121.92, 121.88, 120.78, 119.35, 109.32, 70.53, 24.83. Mass (EI): m/z 250 (M^+), 251 ($M + H^+$), 249 ($M - H^+$).

Ethyl 8-Butanoateoxy-2-methyl-quinoline (4). Yield: 95%. ^1H NMR (400 MHz, CD_3Cl, ppm): δ 8.00 (1H, d, J = 8.41 Hz), 7.39−7.35 (2H, m), 7.28 (1H, t, J = 8.09 Hz), 7.08 (1H, d, J = 6.47 Hz), 4.31 (2H, t, J = 6.79 Hz), 4.16 (2H, q, J = 7.12 Hz), 2.78 (3H, s), 2.62 (2H, t, J = 7.12 Hz), 2.33 (2H, m), 1.25 (3H, t, J = 7.44 Hz). ^{13}C NMR (75 MHz, $CDCl_3$, ppm): δ 172.91, 157.69,

(8) Goldsmith, C. R.; Lippard, S. J. *Inorg. Chem.* **2006**, *45*, 555.
(9) Henary, M. M.; Wu, Y.; Fahrni, C. J. *Chem.—Eur. J.* **2004**, *10*, 3015.
(10) Shults, M. D.; Pearce, D. A.; Imperiali, B. *J. Am. Chem. Soc.* **2003**, *125*, 10591.
(11) van Dongen, E. M. W. M.; Dekkers, L. M.; Spijker, K.; Meijer, E. W.; Klomp, L. W. J.; Merkx, M. *J. Am. Chem. Soc.* **2006**, *128*, 10754. (b) van Dongen, E. M. W. M.; Evers, T. H.; Dekkers, L. M.; Meijer, E. W.; Klomp, L. W. J.; Merkx, M. *J. Am. Chem. Soc.* **2007**, *129*, 3494.
(12) Wang, H.-H.; Gan, Q.; Wang, X.-J.; Xue, L.; Liu, S.-H.; Jiang, H. *Org. Lett.* **2007**, *9*, 4995.
(13) (a) Some selected examples of zinc sensors based on the picolylamine binding moiety: Burdette, S. C.; Lippard, S. J. *Inorg. Chem.* **2002**, *41*, 6816. (b) Burdette, S. C.; Frederickson, C. J.; Bu, W.; Lippard, S. J. *J. Am. Chem. Soc.* **2003**, *125*, 1778. (c) Lim, N. C.; Schuster, J. V.; Porto, M. C.; Tanudra, M. A.; Yao, L.; Freake, H. C.; Brükner, C. *Inorg. Chem.* **2005**, *44*, 2018. (d) Nolan, E. M.; Jaworski, J.; Racine, M. E.; Sheng, M.; Lippard, S.-J. *Inorg. Chem.* **2006**, *45*, 9748. (e) Kiyose, K.; Kojima, H.; Urano, Y.; Nagano, T. *J. Am. Chem. Soc.* **2006**, *128*, 6548. (f) Kim, T. W.; Park, J.-H.; Hong, J.-I. *J. Chem. Soc., Perkin Trans. 2* **2002**, 923.
(14) Nolan, E. M.; Burdette, S. C.; Harvey, J. H.; Hilderbrand, S. A.; Lippard, S. J. *Inorg. Chem.* **2004**, *43*, 2624.
(15) (a) Song, K. C.; Kim, J. S.; Park, S. M.; Chung, K.-C.; Ahn, S.; Chang, S.-K. *Org. Lett.* **2006**, *8*, 3413. (b) Richter, M. M. *Chem. Rev.* **2004**, *104*, 3003. (c) Palacios, M. A.; Wang, Z.; Montes, V. A.; Zyryanov, G. V.; Hausch, B. J.; Jursíková, K. *Chem. Commun.* **2007**, 3708.
(16) (a) Petkova, E. G.; Lampeka, R. D.; Gorichko, M. V.; Domasevitch, K. V. *Polyhedron* **2001**, *20*, 747. (b) Caris, C.; Baret, P.; Pierre, J.-L.; Serratrice, G. *Tetrahedron.* **1996**, *52*, 4659.

153.79, 139.66, 135.73, 127.42, 125.38, 122.16, 119.36, 109.12, 67.61, 60.10, 30.50, 25.44, 23.97, 13.96. Mass (EI): *m/z* 273 (M^+).

General Synthetic Procedure for 6 and 7. A solution of **3** or **4** (1.2 g) in dioxane (20 mL) was heated to 60 °C. To this solution was added SeO_2 (0.65 g). The temperature was then increased to 80 °C. After 2.5 h, the mixture was cooled to ambient temperature. The precipitates were filtered off and washed with dioxane (5 mL) and methylene chloride (5 mL). The organic phases were combined and concentrated to give a crude product. The pure product was obtained by flash chromatography (silica gel) or recrystallization.

8-Pyridylmethyloxy-quinoline-2-carbaldehyde (6). Recrystallization from ethyl acetate and hexane. Yield: 72%. ^{1}H NMR (400 MHz, $CDCl_3$, ppm): δ 10.34 (1H, s), 8.64 (1H, d, J = 4.50 Hz), 8.30 (1H, d, J = 8.62 Hz), 8.10 (1H, d, J = 8.43 Hz), 7.72 (2H, br), 7.57−7.47 (2H, m), 7.26−7.23 (1H, m), 7.19 (1H, d, J = 7.66 Hz), 5.69 (2H, s). ^{13}C NMR (100 MHz, $CDCl_3$, ppm): δ 193.93, 156.88, 154.94, 151.72, 149.36, 140.25, 137.41, 137.13, 131.52, 129.79, 122.92, 121.44, 120.27, 118.04, 111.00, 71.80. Mass (EI): *m/z* 264 (M^+), 265 (M + H^+), 263 (M − H^+).

Ethyl 8-Butanoateoxy-quinoline-2-carbaldehyde (7). Chromatography (methylene chloride containing 0–5% ethyl acetate). Yield: 80%. ^{1}H NMR (400 MHz, $CDCl_3$, ppm): δ 10.28 (1H, s), 8.28 (1H, d, J = 8.43 Hz), 8.07 (1H, d, J = 8.43 Hz), 7.60 (1H, t, J = 7.92 Hz), 7.48 (1H, d, J = 8.17 Hz), 7.19 (1H, d, J = 7.66 Hz), 4.37 (2H, t, J = 6.13 Hz), 4.17 (2H, q, J = 7.15 Hz), 2.66 (2H, t, J = 7.15 Hz), 2.36 (2H, m), 1.26 (3H, t, J = 7.15 Hz). ^{13}C NMR (75 MHz, $CDCl_3$, ppm): δ 193.84, 173.12, 155.38, 151.43, 140.13, 137.24, 131.38, 129.79, 119.71, 117.78, 110.04, 68.18, 60.51, 30.69, 24.27, 14.24. Mass (EI): *m/z* 287 (M^+), 288 (M + H^+).

General Synthetic Procedure for HQ1, HQ3, and 8. To a mixture of aldehydes (**5–7**, 1.5 mmol) and di-2-picolylamine (0.3 g, 1.5 mmol) in 1, 2-dichloroethane (10 mL) was added $NaBH(OAc)_3$ (0.41 g, 2 mmol) in portions. The resulting solution was stirred at room temperature overnight. The solution was first acidified with 1 N HCl to pH 4–5, then neutralized with 1 N NaOH to pH 7–8. The organic phase was separated, and the aqueous phase was extracted with dichloromethane (DCM, 3 × 10 mL). The organic phases were combined and dried over Na_2SO_4. The solvents were evaporated to give a crude product, which was purified by flash chromatography (silica gel) to give the desired products.

Bis(2-pyridylmethyl)(8-benzyloxy-quinoline-2-methyl)amine (HQ1). Chromatography (methylene chloride containing 0–2% methanol). Yield: 96%. ^{1}H NMR (300 MHz, $CDCl_3$, ppm): δ 8.55 (2H, d, J = 4.54 Hz), 8.11 (1H, d, J = 8.55 Hz), 7.80 (1H, d, J = 8.46 Hz), 7.68−7.52 (6H, m), 7.38−7.28 (5H, m), 7.15−7.02 (3H, m), 5.44 (2H, s), 4.11 (2H, s), 3.95 (4H, s). ^{13}C NMR (100 MHz, $CDCl_3$, ppm): δ 159.33, 159.04, 154.22, 149.05, 139.93, 137.23, 136.44, 136.36, 128.59, 128.53, 127.69, 127.04, 126.13, 123.24, 122.02, 121.44, 119.91, 110.62, 70.87, 60.56, 60.15. Mass (ESI-MS): *m/z* 447.4 (M + H^+), 469.3 (M + Na^+), 485.3 (M + K^+).

Bis(2-pyridylmethyl)(8-pyridylmethyloxy-quinoline-2-methyl)-amine (HQ3). Recrystallization from ethyl ether. Yield: 80%. ^{1}H NMR (400 MHz, $CDCl_3$, ppm): δ 8.61 (1H, d, J = 4.71 Hz), 8.55 (2H, d, J = 4.71 Hz), 8.12 (1H, d, J = 8.57 Hz), 7.84 (1H, d, J = 8.43 Hz), 7.72−7.63 (6H, m), 7.38−7.31 (2H, m), 7.21 (1H, t, J = 5.71 Hz), 7.14−7.12 (2H, m), 7.06−7.04 (1H, m), 5.53 (2H, s), 4.15 (2H, s), 3.96 (4H, s). ^{13}C NMR (100 MHz, $CDCl_3$, ppm): δ 159.40, 157.48, 153.87, 149.09, 149.06, 139.75, 136.93, 136.45, 128.65, 126.17, 123.14, 122.57, 122.06, 121.45, 121.35, 120.09, 71.50, 60.87, 60.29. Mass (MALDI-TOF): *m/z* 447.9 (M + H^+), 469.9 (M + Na^+).

Bis(2-pyridylmethyl) Ethyl (8-Butanoateoxy-quinoline-2-methyl)amine (8). Chromatography (methylene chloride containing 0–5% methanol). Yield: 76%. ^{1}H NMR (400 MHz, $CDCl_3$, ppm): δ 8.51 (2H, d, J = 4.37 Hz), 8.06 (1H, d, J = 8.51 Hz), 7.75 (1H, d, J = 8.51 Hz), 7.63−7.61 (4H, m), 7.37−7.31 (2H, m), 7.12−7.08 (2H, m), 7.04 (1H, d, J = 6.90 Hz), 4.27 (2H, t, J = 6.21 Hz), 4.10 (2H, q, J = 7.13 Hz), 4.05 (2H, s), 3.91 (4H, s), 2.60 (2H, t, J = 7.13 Hz), 2.28 (2H, m), 1.19 (3H, t, J = 7.13 Hz). ^{13}C NMR (100 MHz, $CDCl_3$, ppm): δ 173.17, 159.31, 158.88, 154.39, 149.06, 139.81, 136.32, 128.51, 126.15, 123.12, 121.94, 121.29, 119.62, 109.65, 67.95, 60.39, 60.32, 60.11, 30.73, 24.34, 14.17. Mass (EI): *m/z* 470 (M^+).

Bis(2-pyridylmethyl)(8-hydroxy-quinoline-2-methyl)amine (HQ2). To a 37% HCl solution (5 mL) was added **HQ1** (0.45 g, 1 mmol). The mixture was heated at 60 °C for 30 min. After cooling, the solution was neutralized with 1 N NaOH to pH 4–5 and then extracted with DCM (3 × 10 mL). The organic phases were combined and dried over Na_2SO_4. The filtrate was evaporated to generate crude residue, which was purified by chromatography (silica gel, DCM/0–2% methanol) to give a brown oil (0.3 g, 84%). ^{1}H NMR (400 MHz, $CDCl_3$, ppm): δ 8.58 (2H, d, J = 4.67 Hz), 8.10 (1H, d, J = 8.52 Hz), 7.66−7.56 (5H, m), 7.42−7.38 (1H, m), 7.29 (1H, d, J = 7.56 Hz), 7.17−7.14 (3H, m), 4.03 (2H, s), 3.95 (4H, s). ^{13}C NMR (75 MHz, $CDCl_3$, ppm): δ 158.99, 156.86, 152.17, 149.0, 137.35, 136.28, 136.15, 127.21, 127.16, 123.02, 121.96, 121.60, 117.25, 109.89, 60.0, 59.41. Mass (ESI-MS): *m/z* 357.2 (M + H^+), 379.2 (M + Na^+).

Sodium Bis(2-pyridylmethyl)(8-butanoateoxy-quinoline-2-methyl)amine (HQ4). This compound was prepared according to our previously reported procedure.[12] Yield: 90%. ^{1}H NMR (400 MHz, DMSO-d_6, ppm): δ 8.51(2H, s), 8.26 (1H, d, J = 8.05 Hz), 7.81−7.67 (5H, m), 7.42 (2H, d, J = 3.58 Hz), 7.26−7.17 (3H, m), 4.17 (2H, s), 3.93 (2H, s), 3.80 (4H, s), 2.16 (2H, s), 2.04 (2H, s). Mass (ESI-MS): *m/z* 465.3 (M + H^+), 487.3 (M + Na^+).

General Synthetic Procedures for Zinc Complexes of HQ's and Their Crystals. HQ's (18 mg) were dissolved in 6 mL of methanol or acetonitrile containing 10% water. To this solution was added $Zn(ClO_4)_2$ (1 equiv) at room temperature. The mixture was shaken for 10 min. An aliquot of the above complex solution (1.0 mL) was drawn out and placed into a glass tube. The precipitating solvents (ethyl acetate or ethyl ether) were then added carefully into the tube. After several days, crystals of zinc complexes of **HQ1** and **HQ2–4** appeared in acetonitrile/water/ethyl ether and methanol/water/ethyl acetate, respectively, and were ready for X-ray diffraction.

Zinc Complex of HQ1 (ZnHQ1). ^{1}H NMR (300 MHz, DMSO-d_6, ppm): δ 8.61 (2H, s), 8.45 (1H, d, J = 8.48 Hz), 7.91 (2H, t, J = 7.44 Hz), 7.26−7.53 (5H, m), 7.36 (8H, s), 5.47 (2H, s), 4.56 (2H, d, J = 16.00 Hz), 4.10 (4H, t, J = 16.09 Hz).

Zinc Complex of HQ2 (ZnHQ2). ^{1}H NMR (400 MHz, DMSO-d_6, ppm): δ 8.59 (2H, d, J = 11.01 Hz), 8.41 (1H, d, J = 8.81 Hz), 8.02 (2H, t, J = 7.34 Hz), 7.60 (2H, d, J = 8.08 Hz), 7.51−7.34 (6H, m), 4.54 (4H, m), 4.39 (2H, s).

Zinc Complex of HQ3 (ZnHQ3). ^{1}H NMR (300 MHz, DMSO-d_6, ppm): δ 8.71 (1H, d, J = 8.20 Hz), 8.26 (1H, t, J = 7.62 Hz), 8.09−7.93 (4H, m), 7.86−7.80 (5H, m), 7.76−7.67 (3H, m), 7.50 (1H, t, J = 6.28 Hz), 7.39 (2H, t, J = 6.28 Hz), 6.10 (2H, s), 4.74 (2H, d, J = 16.73 Hz), 4.45 (4H, t, J = 17.28 Hz).

Zinc Complex of HQ4 (ZnHQ4). ^{1}H NMR (400 MHz, DMSO-d_6, ppm): δ 9.03 (2H, s), 8.57 (1H, d, J = 7.42 Hz), 8.05 (2H, s), 7.59−7.55 (7H, m), 7.37 (1H, s), 4.68 (2H, s), 4.41 (2H, s), 4.22 (4H, s), 2.40 (2H, s), 2.22 (2H, s).

Spectroscopic Measurements. Pure water (resistivity 18.2 Ω) was used to prepare all aqueous solutions. The 2.5 mM **HQ** sensors stock solutions in DMSO were stored at 4 °C and thawed before use. The 0.5 M zinc stock solutions were prepared in water. All

Scheme 1. Synthesis of Sensors[a]

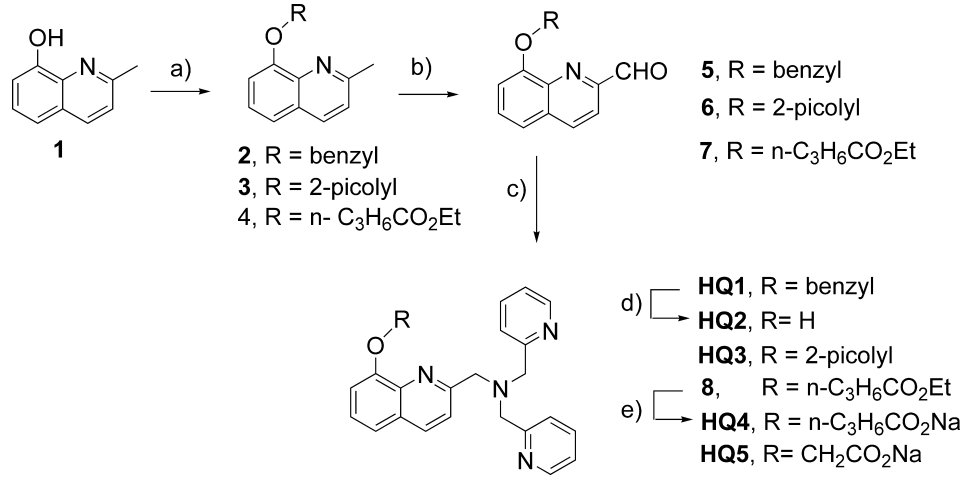

[a] (a) RX, KI /K_2CO_3, acetone, reflux, 24 h. (b) SeO_2, dioxane, 80°C, 2.5 h. (c) Di-2-picolylamine, $NaB(OAc)_3H$, 1,2-dichloroethane, rt, overnight. (d) 37% HCl, 60 °C, 30 min. (e) NaOH 2.5 equiv, rt, 3 h.

fluorescence and UV–vis experiments were carried out in a HEPES buffer containing 5% (v/v) DMSO (25 mM HEPES, 0.1 M $NaClO_4$, pH 7.4).[17] Fluorescence spectra were measured from 330 to 600 nm, and the emissions were integrated from 340 to 590 nm. Quantum yields of the metal-free ligands were measured in a HEPES buffer containing 25 μM EDTA. Quantum yields of metal-bound ligands were measured by using a dilute sample of **HQ**'s (5 μM) and $Zn(ClO_4)_2$ (5 μM). Quinine sulfate in 0.1 N H_2SO_4 (Φ = 0.54)[18] was used as the standard.

Dissociation Constant Determination. Fluorescence intensities of 5 μM **HQ**'s as a function of the free Zn^{2+} concentration were measured in a HEPES buffer. Free Zn^{2+} concentrations were obtained by using a 10.15 mM TNA/0–9 mM $Zn(ClO_4)_2$ buffer system for **HQ1**, 1.1 mM HEDTA/0–1 mM $Zn(ClO_4)_2$ for **HQ3**, and 10 mM EGTA/0–6.25 mM $Zn(ClO_4)_2$ for **HQ4**. The solutions were allowed to equilibrate at 25 °C for 5 min after each addition. The fluorescence intensity data were fitted with eq 1 to calculate K_d in a 1:1 binding model[19]

$$F = \frac{[Zn^{2+}]_{free}F_{max} + K_dF_{min}}{K_d + [Zn^{2+}]_{free}} \quad (1)$$

where F = fluorescence intensity, K_d = dissociation constant, F_{min} = fluorescence intensity of the free ligand, F_{max} = fluorescence intensity of the zinc-loaded sensor, and $[Zn^{2+}]_{free}$ is the free Zn^{2+} concentration.

Metal Ion Selectivity. The fluorescent spectra of a 2 mL aliquot of 5 μM **HQ**'s were acquired in a HEPES buffer after the addition of an aliquot of metal stock solutions (the final metals concentrations are 1.0 mM for $MgCl_2$, $CaCl_2$, and KCl and 5 μM for $MnCl_2$, $FeCl_2$, $CoCl_2$, $NiCl_2$, $CuCl_2$, and $CdCl_2$). After acquisition, an aliquot of $Zn(ClO_4)_2$ (10 μL, 1 mM) was further titrated into related solutions, and the fluorescence of competing samples was measured again.

Crystallography. Measurements were done on a Rigaku RAXIS-RAPID imaging plate diffractometer equipped with a CCD detector using Mo Kα monochromatized radiation (λ = 0.710 73 Å). Cell refinement and data reduction were accomplished by the RAPID AUTO program. The structure was then solved with direct methods and refined using the SHELXL-97 software package.[20] All non-hydrogen atoms were refined anisotropically. Positions of hydrogen atoms attached to carbon atoms were fixed at their ideal positions, and the hydrogens of free water in **ZnHQ1** and **ZnHQ3** were not found in the different maps; therefore, the relevant oxygen atoms were left to be isolated.

Results and Discussion

1. Synthesis. The synthetic routes of sensor **HQ**'s are similar to that of **HQ5** (Scheme 1), which involved three major reactions: the alkylation of **8**-**HQ**, the oxidation of the methyl group to an aldehyde, and the subsequent reductive amination. Accordingly, compounds **2**, **3**, and **4** were prepared by refluxing **8**-**HQ** with alkyl halides in the presence of K_2CO_3/KI. The methyl groups in compounds **2**, **3**, and **4** were further oxidized to generate aldehydes **5**–**7**. The combination of aldehydes and DPA in dry 1,2-dichloroethane in the presence of $NaB(OAc)_3H$ gave **HQ1**, **HQ3**, and **8** in reasonable yields after flash chromatography. Removal of the benzyl group of **HQ1** under concentrated HCl generated **HQ2**. Saponification of the ester, **8**, in the presence of sodium hydroxide gave **HQ4**. Initially, we tried to synthesize **HQ3** and **8** by direct alkylation of **HQ2**; however, the yields of alkylation were very poor, which may be ascribed to the presence of the DPA moiety. Finally, the zinc complexes of each ligand were obtained through reaction of the sensors with zinc perchlorate. The suitable single crystals of **ZnHQ**'s were obtained from the mixed solvents. All compounds were characterized by ^{1}H NMR, ^{13}C NMR,

(17) 5% DMSO was used to increase the solubility of **HQ1** and **HQ3** in an aqueous buffer. Although the other sensors are water-soluble, all measurements were done in 5% DMSO for consistency. A control experiment based on **HQ5** was conducted to re-evaluate its dissociation binding in the presence of 5% DMSO. We found that the dissociation bindings of **HQ5** in the absence and presence of 5% DMSO were very close. Therefore, we concluded that DMSO did not affect the dissociation constants of HQs under the present conditions. In addition, similar conditions were used by: O'Halloran, T. V. *J. Am. Chem. Soc.* **2004**, *126*, 712.

(18) Demas, J. N.; Grosby, G. A. *J. Phys. Chem.* **1971**, *75*, 991.

(19) Hirano, T.; Kikuchi, K.; Urano, Y.; Nagano, T. *J. Am. Chem. Soc.* **2002**, *124*, 6555.

(20) (a) Sheldrick, G. M. *SHELXS97, Program for Crystal Structure Determination*; University of Göttingen: Göttingen, Germany, 1997. (b) Sheldrick, G. M. *SHELXL97, Program for Crystal Structure Refinement*; University of Göttingen: Göttingen, Germany, 1997.

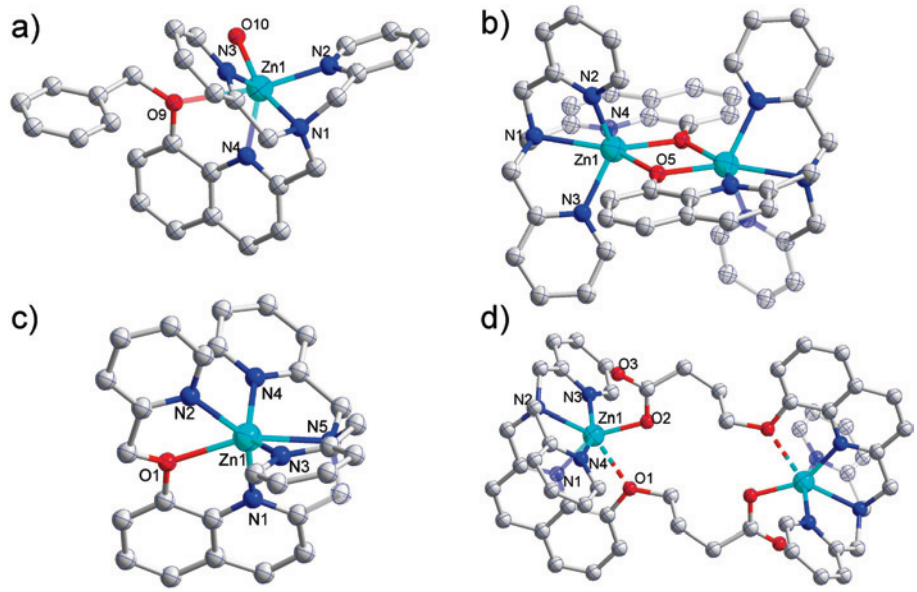

Figure 1. Crystal structures of zinc complexes with **HQ**'s: (a) **ZnHQ1**, (b) **ZnHQ2**, (c) **ZnHQ3**, and (d) **ZnHQ4**. Hydrogen atoms and solvents are omitted for clarity. Red, oxygen; dark blue, nitrogen; light blue, zinc; white, carbon.

Table 1. Crystallographic Parameters for Complexes **ZnHQ**'s

compound	**ZnHQ1**	**ZnHQ2**	**ZnHQ3**	**ZnHQ4**
formula	$C_{58}H_{62}N_8O_{23}Cl_4Zn_2$	$C_{44}H_{38}N_8O_{10}Cl_2Zn_2$	$C_{28}H_{26}N_5O_{9.5}Cl_2Zn$	$C_{52}H_{54}N_8O_{16}Cl_2Zn_2$
solvent systems	CH_3CN/H_2O /ethyl ether	CH_3OH/H_2O /ethyl acetate	CH_3OH/H_2O /ethyl acetate	CH_3OH/H_2O /ethyl acetate
fw	1511.70	1040.50	720.81	1248.67
wavelength (å)	0.71073	0.71073	0.71073	0.71073
cryst syst	monoclinic	monoclinic	monoclinic	monoclinic
space group	*Cc*	$P2_1/c$	*C*2/*c*	$P2_1/c$
T (K)	113(2)	273(2)	298(2)	298(2)
a (Å)	18.152(4)	9.1049(3)	24.382(9)	12.819(3)
b (Å)	10.912(2)	10.2862(3)	14.017(3)	13.847(3)
c (Å)	16.325(3)	23.2337(7)	19.657(11)	15.530(3)
β (deg)	92.56(3)	91.900(2)	115.36(4)	99.67(3)
V (Å^3)	3230.5(11)	2174.75(12)	6071(4)	2717.5(9)
Z	2	2	8	2
D (mg/m^{-3})	1.554	1.589	1.577	1.526
F(000)	1556	1064	2952	1288
μ (Mo *K*a) (mm^{-1})	0.993	1.296	1.049	1.059
θ range (deg)	2.18∼27.90	1.75∼28.32	2.25∼25.00	1.61∼27.48
goodness of fit on F^2	1.024	1.026	1.208	1.146
R_1, wR_2 [$I > 2\sigma(I)$][a]	0.0558, 0.1392	0.0754, 0.1580	0.0813, 0.1664	0.0945, 0.1781
R indices (all data)	0.0681, 0.1477	0.1514, 0.1953	0.1077, 0.1773	0.1668, 0.2099

[a] $R = \sum||F_o| - |F_c||/\sum|F_o|$, $wR_2 = \{\sum[w(F_o^2 - F_c^2)^2]/\sum[w(F_o^2)^2]\}^{1/2}$.

and MS (see the Supporting Information). The complexes were also analyzed by X-ray diffraction.

2. X-Ray Structures. Single crystal structures and data for **ZnHQ**'s are shown in Figure 1 and Table 1, respectively. As shown in Figure 1a, the zinc ion in **ZnHQ1** was wrapped by three pyridyl groups to form a classical DPA-based conformation, as observed in other Zn−DPA complexes.[12,21] The benzyl group was placed in an almost perpendicular position relative to the quinoline ring. The distance of phenolic O(9) to Zn(1) at 2.688(4) Å—obviously longer than that in other complexes, such as 2.391(3) Å (O(1)−Zn(1)) in **ZnHQ5**[12]—is indicative of a weak coordination. In addition, one water molecule was found coordinated to the zinc ion to complete the distorted six-coordination geometry. Another crystal structure of **ZnHQ1** was also obtained from a mixture of water/methanol (Figure S1, Supporting Information). In both crystal structures, zinc ions adopted similar coordination geometry, except in one case where a perchlorate ion instead of one water molecule was found coordinated to the zinc ion. The crystal structure of **ZnHQ3** revealed that the pendant pyridyl group at the 8 position participated in zinc coordinations (Figure 1c), which simultaneously enhanced the interaction between Zn(1) and O(1) (2.318(4) Å) and eventually led to the very high affinity. We expected that the crystal structure of **ZnHQ4** would resemble that of **ZnHQ5**, in which the carboxylic group and zinc ion formed an intramolecular Zn−O bond.[12] To our surprise, the crystal

(21) (a) Burdette, S. C.; Walkup, G. K.; Springler, B.; Tsien, R. Y.; Lippard, S. J. *J. Am. Chem. Soc.* **2001**, *123*, 7831. (b) Burdette, S. C.; Frederickson, C. J.; Bu, W.; Lippard, S. J. *J. Am. Chem. Soc.* **2003**, *125*, 1778. (c) Royzen, M.; Durandin, A.; Young, V. C., Jr.; Geacintov, N. E.; Canary, J. W. *J. Am. Chem. Soc.* **2006**, *128*, 3854. (d) Trosch, A.; Vahrenkamp, H. *Eur. J. Inorg. Chem.* **1998**, 827. (e) Mikata, Y.; Wakamatsu, M.; Yano, S. *Dalton Trans.* **2005**, 545. (f) McDonough, M. J.; Reynolds, A. J.; Lee, W. Y. G.; Jolliffe, K. A. *Chem. Commun.* **2006**, 2971.

Table 2. Spectroscopic Properties and Dissociation Constants for **HQ**'s and **ZnHQ**'s[a]

		absorption maxima		emission maxima		fluorescence quantum yields	
		λ (nm), $\varepsilon \times 10^4$ ($M^{-1}cm^{-1}$)		λ (nm)		Φ[b]	
	K_d for Zn^{2+}	free ligand	Zn^{2+} complex	free ligand	Zn^{2+} complex	free ligand	Zn^{2+} complex
HQ1	1.38 nM	245, 3.74	250, 3.84	445	455	0.029	0.24
HQ2	18.8 fM[c]	244, 3.99	256, 3.73	N.D.[d]	N.D.[d]	N.D.[d]	N.D.[d]
HQ3	0.85 pM	244, 3.75	245, 3.94	429	430	0.022	0.49
HQ4	0.17 nM	245, 5.29	250, 5.35	450	460	0.090	0.65
HQ5[e]	0.45 fM	244, 4.07	245, 3.96	425	438	0.030	0.43

[a] All spectroscopic measurements were performed in 25 mM HEPES, 0.1 M $NaClO_4$, and a 5% (v/v) DMSO pH 7.4 buffer. [b] Quinine sulfate ($\Phi = 0.54$ in 0.1 N H_2SO_4) was used as the standard for quantum yield measurements. The quantum yields of free ligands were measured in the presence of EDTA. [c] The K_d value of HQ2 was measured by fitting UV absorbance ($\lambda = 256$ nm) versus the free Zn^{2+} concentrations (see Supporting Information). [d] Not determined due to the nonfluorescence of HQ2. [e] See ref 12.

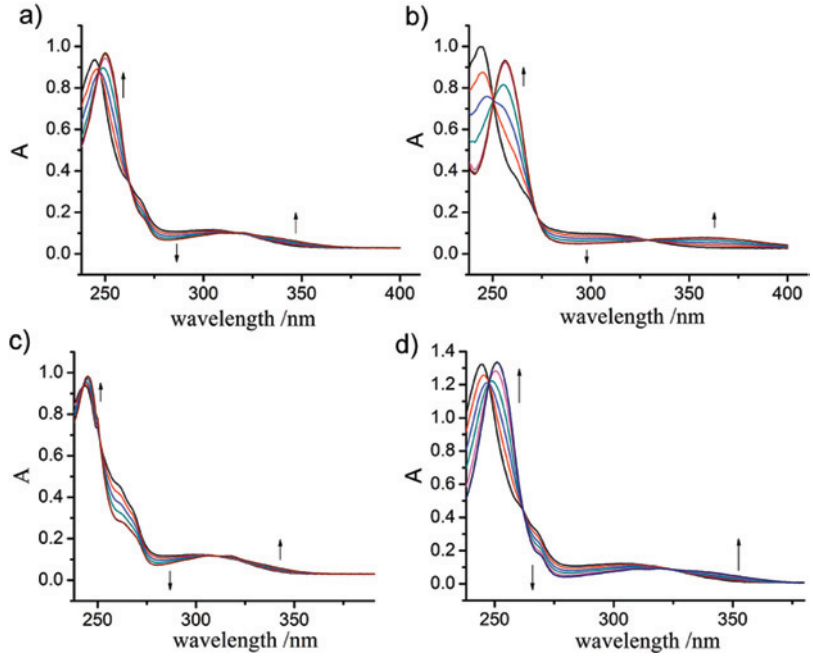

Figure 2. UV–vis spectra of **HQ**'s (25 μM). (a) **HQ1**, (b) **HQ2**, (c) **HQ3**, and (d) **HQ4** upon the titration of Zn^{2+} (0.2, 0.4, 0.6, 0.8, 1.0, 1.2, and 1.6 equiv) in a HEPES buffer.

structure of **ZnHQ4** revealed that one butylcarboxylic group in one ligand was coordinated to the zinc ion sequestered in the other ligand and consequently resulted in a dinuclear structure rather than a mononuclear structure (Figure 1d). The bonds between carboxylic groups and zinc ions (1.977(4) Å) in the crystal structure of **ZnHQ4** are very close to those (2.033(3) Å) in **ZnHQ5**; whereas, the bond Zn(1)–O(1) (2.514(4) Å) in **ZnHQ4** is slightly longer than that (2.425(3) Å) in **ZnHQ5**. This was due to the butylcarboxylic group preferred to adopt a less-strained conformation than its acetocarboxylic counterpart. **ZnHQ2** also exhibited an unexpected dinuclear zinc structure (Figure 1b) in which zinc ions were chelated by the two parallel quinoline rings and bridged by phenolic oxygen atoms to form an almost planar dinuclear unit. Four pyridyl fragments bound to Zn^{2+} at the peripheral position from quinoline rings and were separated at both sides of the dinuclear unit plane. All bond distances of nitrogen atoms to zinc varied in the normal range,[12,20] except for that of Zn(1)−N(1) (2.433(5) Å). We presume the formation of the dinuclear unit occurs partially because the phenolic oxygen atoms in **ZnHQ2** are able to act as two binding sites for zinc ions and partially because the deprotonation of phenol and the subsequent formation of a negatively charged group significantly enhance its affinity for zinc ions. This can be concluded from the fact that the bond distances of Zn–O (2.126(4) and 2.149(4) Å) in **ZnHQ2** are significantly shorter than those (2.318–2.688 Å) in the other **ZnHQ**'s.

3. Photophysical Properties. The photophysical properties of **HQ**'s are summarized in Table 2. **HQ1** has a maximal absorption peak at 244 nm and a broad shoulder band in the longer wavelengths before titration under physiological conditions (Figure 2a). Upon the addition of Zn^{2+} (0–1 equiv), the absorbance at 244 nm decreased, accompanied by a new peak at 250 nm, with a significant increase in the absorbance, and a moderate reduction in the absorbance of the broadband around 270 nm was observed. Meanwhile, another new broad absorption peak appeared at 320 nm and tailed out to 370 nm, which could be attributed to the interaction between the quinoline moiety and zinc.[22] As expected, the UV–vis spectra of **HQ1–4** showed a similar tendency to that of **HQ5**[12] but with different extents of variation in the absorbance upon titration of the zinc ions. For example, the UV–vis spectra of **HQ2** exhibited dramatic

(22) Hanaoka, K.; Kikuchi, K.; Kojima, H.; Urano, Y.; Nagano, T. *Angew. Chem., Int. Ed.* **2003**, *42*, 2996.

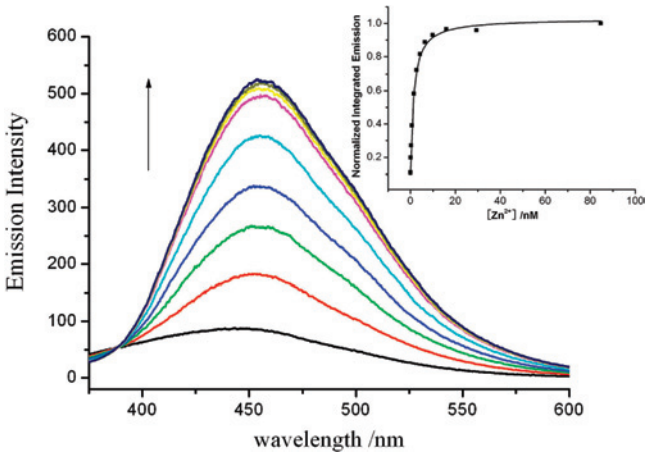

Figure 3. Fluorescence spectra (λ_{ex} = 320 nm) of 5 μM **HQ1** upon the titration of Zn^{2+} (0.2, 0.4, 0.6, 0.8, 1.0, 1.2, and 1.6 equiv) in a HEPES buffer. Insert: fluorescence intensity as a function of Zn^{2+} concentration.

variation at 244 and 256 nm, which can be attributed to the deprotonation of phenol. In contrast, **HQ3** experienced a slight change around 250 nm upon the addition of zinc ions. Moreover, all display three isosbestic points (Figure 2), which indicate the formation of only one UV-active zinc complex. In addition, the saturated spectra were readily obtained when 1 equiv of Zn^{2+} was introduced, suggesting strong affinity for zinc ions and the formation of 1:1 adducts with Zn^{2+}. The latter were further confirmed by Job's plot (see the Supporting Information).

The fluorescence spectra of **HQ1**, **HQ3**, and **HQ4** are shown in Figure 3 and Figure S2 of the Supporting Information. Under simulated physiological conditions, **HQ1**, **HQ3**, and **HQ4** exhibited maximum emission around 425∼450 nm with very low quantum yields of 0.029, 0.022, and 0.09, respectively, in the absence of zinc ions (Table 2). Upon the addition of Zn^{2+} (0–1.6 equiv), the fluorescence intensities of **HQ1**, **HQ3**, and **HQ4** showed a 4∼6-fold enhancement with remarkably enhanced quantum yields of 0.24, 0.49, and 0.65, respectively. At the same time, the maximal emission peaks displayed a 5∼10 nm red-shift. It is obvious that the fluorescence enhancement is due to the lone pair of the tertiary nitrogen chelating to the zinc ion and, consequently, preventing PET. The photophysical properties of **HQ1**, **HQ3**, and **HQ4** are comparable with those of **HQ5**, indicative of the variation of pendant groups at the 8 position of quinoline exerting no effect on its photoproperties. Unexpectedly, though the UV–vis spectra of **HQ2** underwent dramatic change (Figure 2b), the fluorescent signals of **HQ2** remained silent while zinc ions were introduced. This phenomenon is distinctly different from those of **HQ2** analogues (Chart 2) as described by Canary et al.[6g,21c] and Aoki et al.[23] Canary et al. reported that **HQ2MS1** and **HQ2MS2** acted as fluorescence "turn-on" sensors for zinc ions. Conversely, Aoki and co-workers observed that **HQ2MS1** worked as a fluorescence "turn-off" sensor for zinc ions. Due to these conflicting results presented

Chart 2. Analogues of **HQ2**

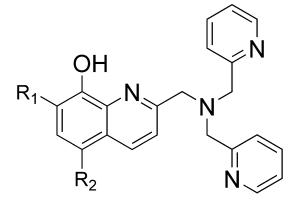

HQ2MS1: R_1=H, R_2=SO_2NMe_2
HQ2MS2: R_1=R_2=SO_2NMe_2

in the literature, we are unable to draw any useful information to interpret the phenomenon of the nonfluorescence of **HQ2**. However, after a careful survey of zinc/DPA complexes' crystal structures,[12,21] we find that the bond distance between zinc and tertiary amino nitrogen (2.433 Å) in **ZnHQ2** is obviously longer than those (2.2–2.3 Å) in the other zinc/DPA complexes, which hints at the feasibility of the PET process involving tertiary amine being not fully shut down even in the presence of zinc ions. This may partially account for the lack of enhanced fluorescence of **HQ2** upon zinc titration.

4. Apparent Zn^{2+} Binding Affinities. Due to the high binding capability of **HQ**'s toward zinc ions, their dissociation constants could not be directly extracted from UV or fluorescence titrations. A reliable approach is to use zinc-ligand buffered solutions, which can provide various and accurate free zinc concentrations. As expected, these sensors showed fluorescence enhancement on a broad range of concentrations, which are higher than that for **HQ5** (Figure 4). Accordingly, a proper zinc/ligand buffer system was carefully chosen for each sensor. In our experiments, the following free zinc buffers were used: zinc/TNA buffer (log K (ZnL) = 10.66 (25 °C, μ = 0.1) and pK_1 = 9.73, pK_2 = 2.49, pK_3 = 1.89) for **HQ1**; zinc/HEDTA buffer (log K (ZnL) = 14.60 (25 °C, μ = 0.1) and pK_1 = 9.87, pK_2 = 5.38, pK_3 = 2.62, pK_4 = 1.60) for **HQ3**; and zinc/EGTA (log K (ZnL) = 12.60 (25 °C, μ = 0.1) and pK_1 = 9.40, pK_2 = 8.79, pK_3 = 2.70) for **HQ4**. Subsequently, the K_d values were calculated to be as follows: 1.38 ± 0.02 nM for **HQ1**, 0.85 ± 0.02 pM for **HQ3**, and 0.17 ± 0.02 nM for **HQ4**

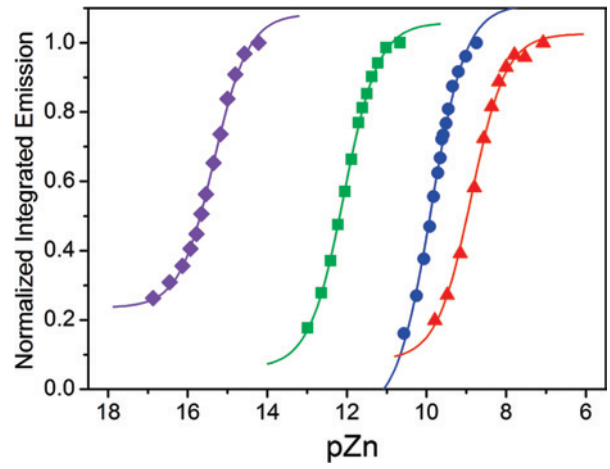

Figure 4. Changes of fluorescence intensities for sensors: **HQ1** (red triangle), **HQ3** (green square), **HQ4** (blue circle), and **HQ5** (violet rhombus) as a function of free Zn^{2+} (pZn = $-\log[Zn^{2+}]_{free}$).

(23) Aoki, S.; Sakurama, K.; Matsuo, N.; Yamada, Y.; Takasawa, R.; Tanuma, S.-I.; Shiro, M.; Takeda, K.; Kimura, E.; *Chem.—Eur. J.* **2006**, *12*, 9066.

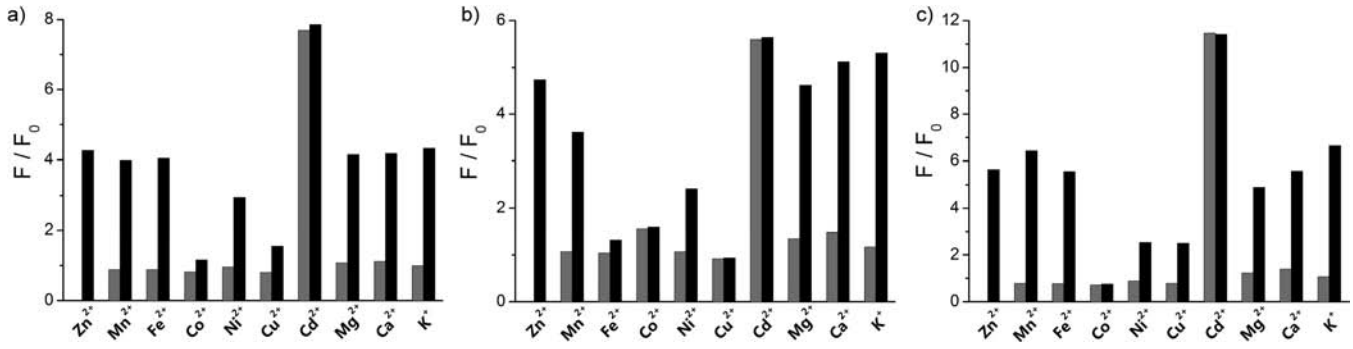

Figure 5. Metal ion selectivity profiles of **HQ**'s (5 μM). (a) **HQ1**, (b) **HQ3**, and (c) **HQ4**: ratio of relative integrated emission between 340 and 590 nm of **HQ**'s + 1 equiv of the indicated metal ions to that of the apoligand (gray bar) and ratio of relative integrated emission of **HQ**'s + 1 equiv of the indicated metal ions, followed by 1 equiv of Zn^{2+}, to that of the apoligand (black bar) in a HEPES buffer.

(Figure 4 and Table 2). The K_d of **HQ1** is about 40-fold smaller than that of a DPA-substituted quinoline sensor (K_d = 59 nM) as reported by Nagano et al.[24] This indicates that incorporation of a benzyloxy group at the 8 position of quinoline has a moderate effect on the affinity of **HQ1**. The crystal structure of **ZnHQ1** revealed that an oxygen atom at the 8 position got involved in the coordination. In addition, NMR titrations also revealed that the chemical shift of O*CH*$_2$Ph shifted to downfield ($\Delta\delta$ = 0.13 ppm) upon titration of 1 equiv of zinc ions (Figure S5, Supporting Information). In contrast, the K_d value of **HQ3** is almost 3 orders of magnitude smaller than that of **HQ1** because the **HQ3** sensor bears one more coordinated site—the picolyl group—than **HQ1**. The chelation of the extra coordinated site to zinc ions was also corroborated by the crystal structure (Figure 1c) and NMR titrations (—*CH*$_2$ pyridyl group downshift up to $\Delta\delta$ = 0.69 ppm, Figure S6, Supporting Information). The K_d of **HQ4** with a butylcarboxylic group is almost 6 orders of magnitude higher than that of **HQ5** (K_d = 0.45 fM) with an acetocarboxylic group, which is due to carboxylic groups in both sensors adopting different chelated conformation (*vide supra*). Recall that **HQ2** is fluorescent-silent, so we are unable to calculate its K_d on the basis of fluorescence titrations. Fortunately, the dramatic change in the UV–vis spectra of **HQ2** upon zinc titration could be utilized to calculate K_d of the **HQ2** sensor. Subsequently, the zinc affinity of 18.8 $\pm$ 0.01 fM for **HQ2** was extracted from the UV–vis spectra via a zinc/HEDTA buffer system (See Supporting Information, Figure S4). This value is comparable with its analogues (Chart 2, log K =13.29 and 14.34).[6g,21c] To the best of our knowledge, small molecule fluorescent sensors with tunable affinities down to the femtomolar range were rarely reported.

5. Selectivity toward Zn^{2+}. Selectivity is always one of the major issues in the field of molecular recognition. It is well-known that DPA, derived from zinc chelator TPEN (= *N*,*N*,*N*′,*N*′-tetrakis(2-pyridylmethyl)ethylene diamine), shows good selectivity for zinc ions over Ca^{2+} and Mg^{2+}. Our recent report revealed that the introduction of an acetocarboxylic group at the 8 position of quinoline did not impair the selectivity of the DPA-substituted sensor.[12] To further evaluate the selectivity of these new sensors, we first measured the fluorescent response in the presence of potential competing metal ions. As expected, the emissions of **HQ1**, **HQ3**, and **HQ4** showed slight enhancement (F/F_0 < 1.2, gray bar in Figure 5) upon the addition of K^+, Mg^{2+}, and Ca^{2+} up to the millimolar range, whereas the fluorescence intensities of **HQ1**, **HQ3**, and **HQ4** were slightly quenched by transition metals (1 equiv) such as Mn^{2+}, Co^{2+}, Fe^{2+}, Ni^{2+}, and Cu^{2+} with the exception of Cd^{2+} showing enhanced fluorescence. The interference of Cd^{2+} was also observed for other zinc fluorescent sensors.[20,24] Considering the coexistence of the zinc ion and the competing metal ions in samples, fluorescent assays for the coexistent systems were repeated. The emission intensities of **HQ1**, **HQ3**, and **HQ4** in the presence of Na^+, K^+, Mg^{2+}, Ca^{2+}, and Mn^{2+} are almost the same as those in the absence of competing metals upon the titration of zinc (Figure 5, black bar). Furthermore, the fluorescence intensities of **HQ1** and **HQ4** were also recovered to the normal level for Fe^{2+}, while Zn^{2+} was titrated. In addition, in the case of Ni^{2+}/Zn^{2+}, the fluorescence intensities of **HQ1**, **HQ3**, and **HQ4** showed a moderate enhancement (F/F_0 is about 3). As observed for other fluorescent sensors for zinc ions,[8,14,25] **HQ1**, **HQ3**, and **HQ4** displayed little or no enhanced fluorescence in the Co^{2+} and Cu^{2+}/Zn^{2+} systems. This is because these two metal ions remain bound and quench their fluorescence even in the presence of 1 equiv of zinc ions. But these ions yield no false-positive signal in the measurement of concentrations of zinc ions because of their fluorescence quenching properties.[25] These results indicate a high selectivity of **HQ** sensors for zinc ions over these competing metals.

Conclusion

We have successfully tuned the affinities of quinoline fluorescent Zn^{2+} sensor **HQ**'s from the subfemtomolar to nanomolar range by varying the pendant ligands. Unlike other tunable systems, our emphasis is to introduce an auxiliary chelating group near the coordination unit rather than to modify the major chelated system. Consequently, the modifications not only exert no effect on the spectroscopic properties of **HQ**'s but also do not impair the selectivity over the competing metal ions under physi-

(24) Hanaoka, K.; Kikuchi, K.; Kojima, H.; Urano, Y.; Nagano, T. *J. Am. Chem. Soc.* **2004**, *126*, 12470.

(25) (a) Lim, N. C.; Brückner, C. *Chem. Commun.* **2004**, 1094. (b) Huang, S.; Clark, R. J.; Zhu, L. *Org. Lett.* **2007**, *9*, 4999.

ological conditions. Although our sensors are able to detect free zinc from the subfemtomolar to nanomolar range, UV excitation is one limiting factor for our sensors, which would hamper their potential biological applications. Thus, developing new zinc fluorescent sensors with excitation wavelength extended to the visible region based on **HQ**'s is a fascinating next project that is currently in progress.

Acknowledgment. We thank the Chinese Academy of Sciences 'Hundred talents program' for financial support. We are grateful to Dr. Jian Wang at The Scripps Research Institute for his critical discussion.

Supporting Information Available: Crystallographic details in CIF format for ZnHQs, additional fluorescence spectra for HQ3 and HQ4, UV–vis titration figure of HQ2, Job's plot, NMR titrations, selected bond distances and bond angles, and ^{1}H and ^{13}C NMR data. This material is available free of charge via the Internet at http://pubs.acs.org.

IC702393Z